Available online at www.garmian.edu.krd

Passer Journal

Passer 6 (Issue 1) (2024) 119-126

http://passer.garmian.edu.krd/

Thermal Radiation Effects on MHD Casson And Maxwell Nanofluids Over a Porous Stretching Surface

Tagallamudi Srinivasa Rao[1], Matam Mohan Babu[2], Ramesh Reddy Bojja[3], Naga Santoshi P[4], Venkata Ramana Reddy Gurrampati[1]*

[1]*Department of Mathematics, Koneru Lakshmaiah Education Foundation, Vaddeswaram, Andhra Pradesh, India-522302.*
[2]*Department of Civil Engineering, Sri Venkatesewara College of Engineering, Chittoor, India-517127.*
[3]*Department of Mathematics, Lakireddy Bali Reddy College of Engineering, Mylavaram, Andhra Pradesh, India-521530.*
[4]*Department of Mathematics, Singareni Collieries Women's Degree & PG College, Kothagudem-507 101.*

Received 13 September 2023; revised 07 January 2024;
accepted 13 February 2023; available online 28 February 2024

DOI: 10.24271/PSR.2024.416203.1389

ABSTRACT

The main goal of the work is to investigate to the influence the magnetohydrodynamic slip flow through a nonlinear porous stretching surface's upper Maxwell Casson convected nanofluid boundary layer flow was considered. The governing partial differential equations are transformed into nonlinear ordinary differential equations using the proper similarity transformations. The Shooting method was utilized to achieve the numerical solution of the updated equations utilizing the Runge-Kutta-Fehlberg approach. A wide range of essential fluid characteristics were thoroughly examined, including the Schmidt number, magnetic parameter, temperature slip parameter, concentration slip parameter, velocity, and nonlinear stretching parameter. Using graphs and tables, the impacts on temperature, concentration, and velocity were examined and reported. The investigation included calculating and thoroughly debating the skin friction coefficient, local Sherwood numbers, and local Nusselt numbers.

Keywords: Casson Fluid Parameter, Maxwell Fluid, Chemical Reaction Parameter, MHD, Slip Effects.

1. Introduction

Potential applications of non-Newtonian fluid flow on porous stretched surfaces include blood flow and engineering. Casson is a liquid that shear thins. It can be a sign of yield stress. When greater yield stress than shear stress is applied, it behaves as a solid; otherwise, it behaves as a liquid and begins to flow. Raju et al[1] investigated the Casson fluid application. Gladys et al[2] Contributions of variable viscosity and thermal conductivity on the dynamics of non-Newtonian nanofluids flow past an accelerating vertical plate. Reddy et al[3] are examined the effect of radiation on MHD mixed convection oscillatory flow over a vertical surface in a porous medium with chemical reaction and thermal radiation. Sandhya et al[4] have analysed the heat and mass transfer effects on MHD flow past an inclined porous plate in the presence of chemical reaction. For the magnetohydrodynamic Carreau and Casson fluids, Kumaran et al.[5] have studied the exponential heat source/sink, momentum, and thermal transport over the spinning paraboloid. A study on free convective heat and mass transfer flow through a highly porous medium with radiation, chemical reaction and Soret effect is analysed by Suneetha et al[6]. Sobamowo et al[6]. have looked at the effects of additional control features on the stream and heat transfer qualities to the nanofluids when the base fluid is implanted with the upper and silver nanoparticles.

Unsteady Carreau-Casson fluids in a solution of dust and graphene nanoparticles with non-Fourier heat flux across a radiating shrinking layer have been explored by Santosh et al.[7]. Santoshi et al.[8] have studied the computational examination of 3D Casson-Carreau nanofluid flow. A colloidal postponement called nano fluid contains nanoparticles in a base fluid. Nano fluids have a wide range of uses in engineering, from the automotive industry to the medical sector. They are used in nuclear reactors, power plant cooling systems, geothermal energy extraction, automotive applications, electronic applications like cooling microchips, and biomedical applications like cancer therapeutics and nano cryosurgery, among other things. Due to these real characteristics, nano fluids are significant to investigate, as shown by the references[9–14] in this debate. The

* Corresponding author
E-mail address: tagallamudi_me@kluniversity.in (Instructor).
Peer-reviewed under the responsibility of the University of Garmian.

non-Newtonian fluid flow across a mixed stretchable surface has been studied with different variables by Chandra and Sandeep[15], Reddy et al.[16], and Tian et al.[17]. Nasir et al.[18] looked at how thermal radiation affected MHD 3D flow across a stretched surface. A nano liquid film's Eyring-Powell slip flow has been studied by Khan et al.[19].

In-depth references[20–26] on this topic examined non-Newtonian Maxwell fluids under a range of physical circumstances, including viscous dissipation, Newtonian heating, homogeneous–heterogeneous chemical interactions, and thermal stratification over a variety of stretching surfaces. They found that when the Prandtl number climbed, both temperature and heat transfer rate dropped. The effect of radiation and convective boundary limitation on the oblique stagnation point of the non-Newtonian nano fluids past the stretching layer was studied by Abuzar et al.[24]. Yasin et al numerical study of the stagnation point flow of nano fluid considers the sloped stretched sheet.

The effects of slip on MHD flow have been studied by certain researchers[25-27] using a variety of non-Newtonian nano fluid models, such as Casson fluid and Jeffery nano-fluid, across a flexible sheet with varied physical limits. Ibrahim et al.[28] investigation of the influence of chemical reaction on mass and heat transport characteristics. Nevertheless, the sources addressing chemical reactions and slip effects are addressed in references[29-48].

The analysis of the MHD stagnation point flow of upper-convected Maxwell fluid with chemical reaction is not considered by any of the researchers due to the impacts of nanoparticles with slip effects. Therefore, using the Runge-Kutta Fehlberg method and the shooting technique, the current paper aims to investigate the impact of nanoparticle and chemical reaction on MHD slip stagnation point flow, boundary layer flow, and heat and mass transfer of upper-convected Casson and Maxwell fluid above a stretching sheet. This work is unusual because it incorporates the influence of nanoparticles with chemical reaction and slip effect in upper-convected MHD Casson and Maxwell fluids.

2. Mathematical Formulation

Consider the 2D motion of a non-Newtonian nano fluid with time dependence and incompressibility, as well as heat radiation and chemical reaction over a porous stretched surface under convective circumstances. The Free stream velocity $u_f(x)$ and the stretching velocity $u_w(x)$ are of the forms $u_f(x) = ax$ and $u_w(x) = bx$ where a and b are constants. The x-axis is along the sheet and normal to the sheet y-axis is chosen. The concentration is represented by C_w and the temperature is represented by T_w and the ambient concentration and ambient temperature are represented by C_∞ and T_∞.

The physical model of the flow and Cartesian coordinates are shown in Fig. 1. The proposed Casson model for two-dimensional laminar steady flow has governing differential equations that are expressed in the following form:

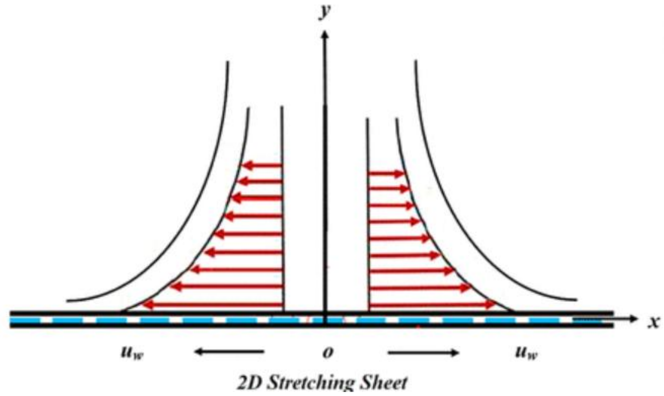

Figure 1: Physical model of the problem.

The flow expressions are defined as[34]

$$\frac{\partial u}{\partial x} + \frac{\partial v}{\partial y} = 0 \tag{1}$$

$$u\frac{\partial u}{\partial x} + v\frac{\partial u}{\partial y} = \left[\left(1+\frac{1}{\gamma}\right)v\frac{\partial^2 u}{\partial y^2} - \varsigma\left(u^2\frac{\partial^2 u}{\partial x^2} + v^2\frac{\partial^2 u}{\partial y^2} + 2uv\frac{\partial^2 u}{\partial x \partial y}\right) + u_f\frac{\partial u_f}{\partial x} - \left(\frac{\sigma B_0^2}{\rho_f} + \frac{\nu}{K_1}\right)(u_l - u)\right] \tag{2}$$

$$u\frac{\partial T}{\partial x} + v\frac{\partial T}{\partial y} = \alpha\frac{\partial^2 T}{\partial y^2} + \tau\left(D_B\frac{\partial C}{\partial y}\frac{\partial T}{\partial y} + \frac{D_T}{T_\infty}\left(\frac{\partial T}{\partial y}\right)^2\right) - \frac{1}{(\rho c_p)_f}\frac{\partial q_r}{\partial y} + \frac{Q_0(T-T_\infty)}{(\rho c_p)_f} \tag{3}$$

$$u\frac{\partial C}{\partial x} + v\frac{\partial C}{\partial y} = D_B\frac{\partial^2 C}{\partial y^2} + \frac{D_r}{T_\infty}\frac{\partial^2 T}{\partial y^2} - K_r(C - C_\infty) \tag{4}$$

The Navier slip conditions, convective conditions and Nield boundary conditions are assumed as follows:

$$u = ax + m_1\frac{\partial u}{\partial y}, v = 0, T = T_w + m_2\frac{\partial T}{\partial y},$$
$$C = C_w + m_3\frac{\partial C}{\partial y} \text{ at } y = 0$$
$$u \to u_e(x) = bx, v \to 0, T \to T_\infty, C \to C_\infty \quad \text{as } y \to \infty \tag{5}$$

where u and v are the velocity components along the x and y directions, ρ_f is the density of the base fluid, $\alpha -$ is the thermal diffusivity, ς is the relaxation time parameter of the fluid, B_0 is the strength of the magnetic field, ν is the kinematic viscosity of the fluid, K_1 is the permeability parameter, γ is the Casson fluid parameter, D_B is the Brownian diffusion coefficient, D_r is the thermophoretic diffusion coefficient, τ is the ratio between the effective heat capacity of the nano particle material and heat capacity of the fluid, C is the volumetric volume expansion coefficient, and ρ is the density of the particle, Kr is the chemical reaction rate, m_1, m_2, and m_3 are the velocity slip, thermal slip and concentration slip conditions respectively..

The radiation heat flux (q_r) is modeled by using Rosseland approximation given in:

$$q_r = -\left(\frac{4\sigma^*}{3k_1}\right)\frac{\partial T^4}{\partial y} \tag{5}$$

Here σ^*represents the constant of Stefan-Boltzmann,k_1 gives the coefficient of mean absorption. It is also assumed that if the difference in temperature within the flow is T^4, then T^4 can be expressed as a linear combination of the temperature by expanding the T^4 by Taylor's series about T_∞ to obtain (7):

$$T^4 = T_\infty^4 + 4T_\infty^3(T - T_\infty) + 5T_\infty^2(T - T_\infty)^2 + \cdots \quad (7)$$

If we neglect the higher order beyond the first degree in $(T - T_\infty)$in this series and opening brackets on the right-hand sides of (7) we obtain (8):

$$T^4 \approx -3T_\infty^4 + 4T_\infty^3 T \quad (8)$$

Substituting the right-hand side of (8) into (5) for T^4yield (9):

$$q_r = -\left(\frac{4\sigma^*}{3k_1}\right)\frac{\partial T^4}{\partial y} = -\left(\frac{4\sigma^*}{3k_1}\right)\frac{\partial}{\partial y}(-3T_\infty^4 + 4T_\infty^3 T) = -\left(\frac{15T_\infty^3\sigma^*}{3k_1}\right)\frac{\partial T}{\partial y} \quad (9)$$

The rate of change in radiative heat flux with respect $y$is given by (13)

$$\frac{\partial q_r}{\partial y} = -\left(\frac{16T_\infty^3\sigma^*}{3k_1}\right)\frac{\partial^2 T}{\partial y^2} \quad (10)$$

The partial differential equations (2),(3),(4) and (5) are transformed into ordinary differential equations by introducing the dimensionless variables are given by (11):

$$\psi = \sqrt{cv}f(\eta), \theta(\eta) = \frac{(T - T_\infty)}{(T_w - T_\infty)}, \phi(\eta) = \frac{(C - C_\infty)}{(C_w - C_\infty)}, \eta = \sqrt{\frac{c}{v}}y \quad (11)$$

The stream function velocity ψ can be defined as$u = \frac{\partial\psi}{\partial y}, v = -\frac{\partial\psi}{\partial x}$so that equation (1) satisfies the continuity equation. $f(\eta)$denote the injection and suction, η is the dimensionless space variable,$\theta(\eta)$ and $\phi(\eta)$are the dimensionless of temperature and concentration of the fluid respectively.

In view of the above-mentioned transformations equations (2), (3) and (48) are reduced to the following ODEs:

$$\left(1 + \frac{1}{\gamma}\right)f''' + ff'' - f'^2 + E^2 + (M + 1/K)(E - f') + \delta(2ff'f'' - f''') = 0 \quad (12)$$

$$\left(1 + \frac{4}{3R}\right)\theta'' + Pr\, f\, \theta' + Pr\, N\, b\phi'\theta' + Nt\theta'^2 + Pr\, Q\, \theta = 0 \quad (13)$$

$$\phi'' + Le\phi' + \frac{Nt}{Nb}\theta'' - KrLe\phi = 0 \quad (14)$$

The transformed boundary restrictions are:

$$f(\eta) = S, f'(\eta) = 1 + L_1 f''(\eta), \theta(\eta) = 1 + L_2\theta'(\eta), \phi(\eta) = 1 + L_3\phi'(\eta) \text{at} \eta = 0$$
$$f'(\eta) \to E, \theta(\eta) \to 0, \phi(\eta) \to 0 \text{as} \eta \to \infty \quad (15)$$

wheref' is dimensionless velocity, θ is dimensionless temperature, $\phi$is dimensionless concentration, and η is the similarity variable. The prime denotes differentiation with respect to η.

The skin friction C_f , local Nusselt number Nu_x and Sherwood number Sh_x are the important physical quantities they can be defined as follows[34]:

$$C_f = \frac{\tau_w}{\rho u_w^2}, Nu_x = \frac{xq_w}{k(T_f - T_\infty)}, Sh_x = \frac{xq_m}{D_B(C_w - C_\infty)}$$

Here $\tau_w = \mu(1 + \beta)\frac{\partial u}{\partial y}$ is the surface shear stress, $q_w = -k\left(\frac{\partial T}{\partial y}\right)_{y=0} + q_r$ is the surface heat flux and $q_m = -D_B\left(\frac{\partial C}{\partial y}\right)_{y=0}$

Using the similarity transformation in (11) we have the following relations:

$$C_f\, Re_x^{\frac{1}{2}} = f'(0), Nu_x\, Re_x^{\frac{-1}{2}} = -\left(1 + \frac{4}{3R}\right)\theta'(0), Sh_x\, Re_x^{\frac{-1}{2}} = -\phi'(0)$$

where Re_x is the local Reynolds number.

3. Numerical Solution

The fourth order Runge-Kutta Fehlberg method based on the shooting scheme is used to solve the system of nonlinear coupled ordinary differential equations (12-14) subject to the boundary constraints (15). This study emphasizes the characteristics of motion, heat, and mass transmission. The field of velocity, energy, and concentration profile, as well as friction factor, Nusselt number, and Sherwood number, are all properly investigated.

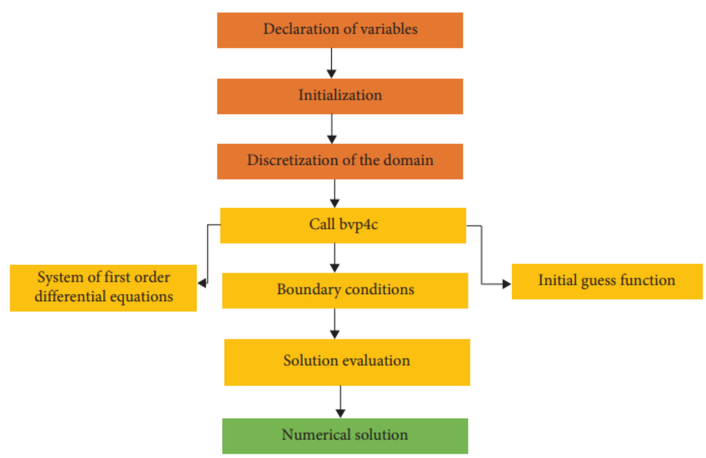

Flow chart of Numerical scheme (BVP4C)

$$f = f(1), f' = f(2); f'' = f(3); \theta = f(4); \theta' = f(5); \phi = f(6); \phi' = f(7);$$
$$f'(3) = f(1)f(3) - f(2)^2 + E^2 + (M + 1/K)(E - f(2)) + \delta(2f(1)f(2)f(3))/(1 + 1/\gamma + \delta)$$
$$f'(5) = -(Pr\, f(1)f(5) + Pr\, N\, bf(7)f(5) + Ntf(5)^2 + Pr\, Q\, f(4))/(1 + (4/3)R)$$

$$f'(7) = -Lef(7) + \frac{Nt}{Nb}\Big(\big(Pr\, f(1)f(5) + Pr\, N\, bf(7)f(5) + Ntf(5)^2 + Pr\, Q\, f(4)\big)/(1+(4/3)R)\Big) - KrLef(6)$$

4. Results and Discussion

In this connection the successive outcomes for physical variables are evaluated M=0.5, β=0.1, $\gamma = 0.2, Pr = 0.71, Le = 1.0, Nb = 0.1, S = 0.5, Nt = 0.1, R = 0.2, Kr = 0.2, Q = 0.1, E = 0.01.$ For this study, the successive outcomes for physical variables are evaluated.

Figure 2 depicts how the magnetic field's properties affect the flow velocity. It has been shown that the magnetic parameter generates the Lorentz force, which causes the fluid's velocity to slow down and the velocity profile to rise to higher magnetic parameter values. Figure 3 shows the variation of velocity profiles for various permeability parameter values (K). It is evident that the presence of a porous media increases the fluid flow's values, which accelerates the fluid. As a result, the influence of increasing permeability parameter values on fluid velocity results in a thickening of the thermal boundary layer.

The fluid's velocity is decreased by the Casson effect in Figure 4. It is crucial because the yield stress of the Casson fluid is lowering. Physically, a decrease in the yield strain appears to be caused by an increase in the Casson parameter, which raises the liquid's plastic dynamic viscosity and thickens the momentum boundary layer.

The temperature curves for various estimates of the thermal radiation parameter are shown in Figure 5. When thermal radiation calculations are improved, it is discovered that the temperature profile and the thickness of the temperature boundary layer rise. When the estimates of Pr were improved and the thermal diffusivity was decreased, the temperature and thermal boundary layer thickness fell, which led to a decrease in the temperature profile, as shown in Figure 6. The relative thickness of momentum and thermal boundary layers is governed by how quickly and slowly heat diffuses depending on Pr.

Figure 7 shows how temperature profiles with increasing Q values improve the thermal boundary layers. When a heat source is present, the energy is delivered to the flow. The energy enhances the thermal boundary layers. The concentration in this figure drops as the thermophoresis parameter values rise.

Figure 8 illustrates how the thermophoresis parameter affects the concentration profiles. As Nt rises, the thermal and concentration boundary layers get thicker. As the temperature and Nb temperature curves in Figure 9. At the surface, the thermal boundary layer's thickness is seen to be increasing.

The concentration profile for various Kr levels is shown in Figure 10. It was observed that the concentration profile decreased with an update to the Kr. This demonstrates how thickening the concentration boundary layer results in a drop in the concentration profile due to an increase in the chemical reaction parameter.

The effect of the Lewis number on concentration profiles is seen in Figure 11. The graphic shows that the thickness of the concentration graph and the concentration border layer decreases with increasing Lewis number values.

For different values of B,Q,Nt,Nb,Kr,Le,L_1,L_2,L_3 and S, the variation of $-f''(0), -\theta'(0)$ and $-\phi'(0)$ is given in Table 1. The table shows that when the suction-injection parameter S and Deborah number grow, the skin friction coefficient rises but falls with an increase in the velocity ratio E and the velocity slip parameter. The table also demonstrates how the local Nusselt number and the local Sherwood number of the flow region change when the values of S and E change in response to changes in Deborah number and velocity slip parameter L_1.

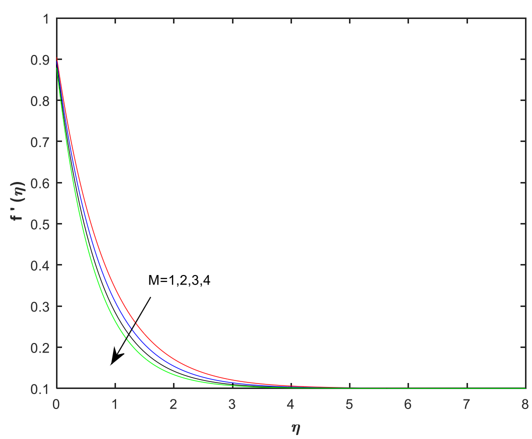

Figure 2: Velocity Profile for various values of M

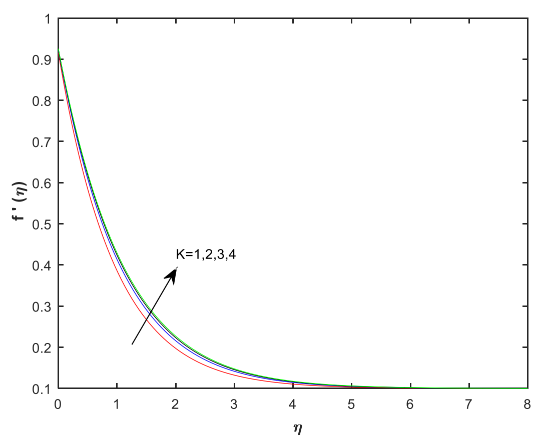

Figure 3: Velocity Profiles for various values of K.

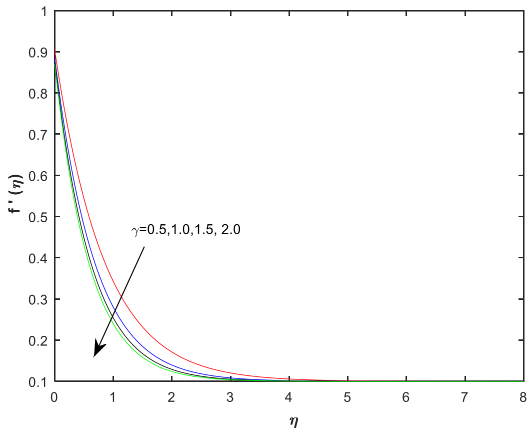

Figure 4: Velocity Profile for various values of γ

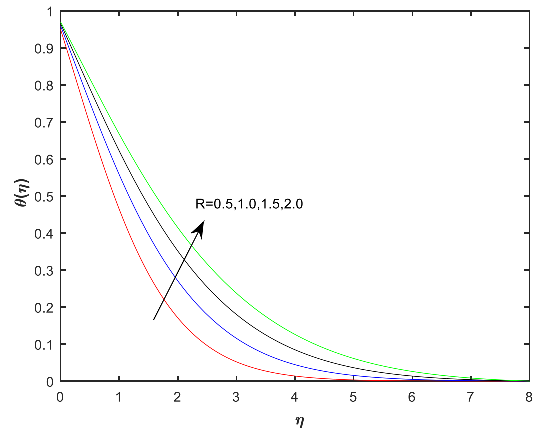

Figure 5: Temperature Profile for various values of R.

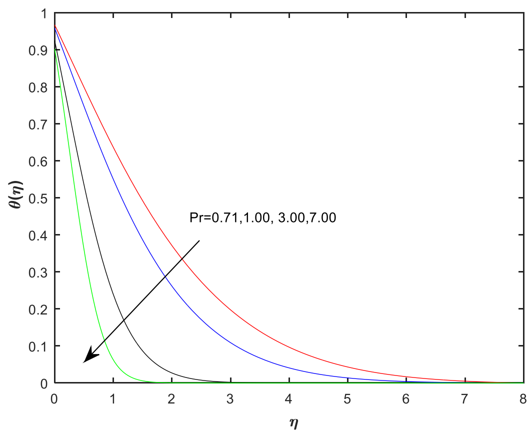

Figure 6: Temperature Profile for various values of Pr.

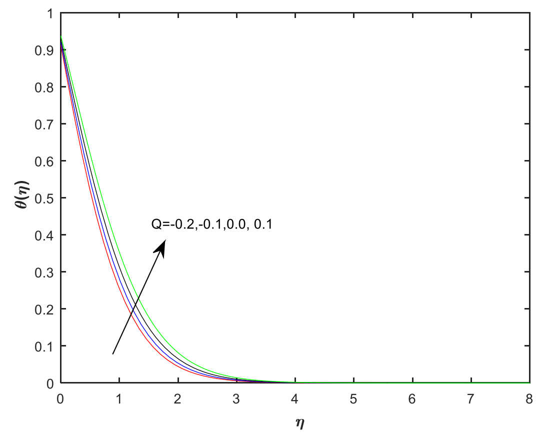

Figure 7: Temperature Profile for various values of Q.

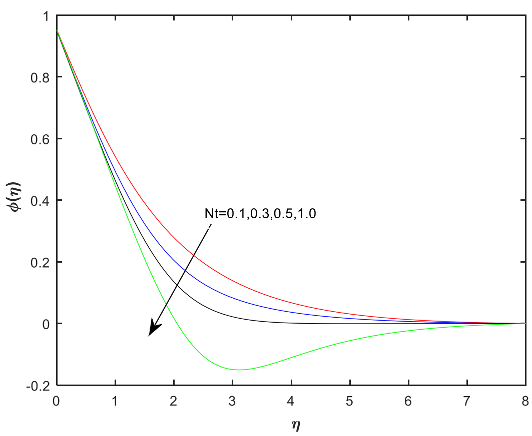

Figure 8: concentration Profile for various values of Nt.

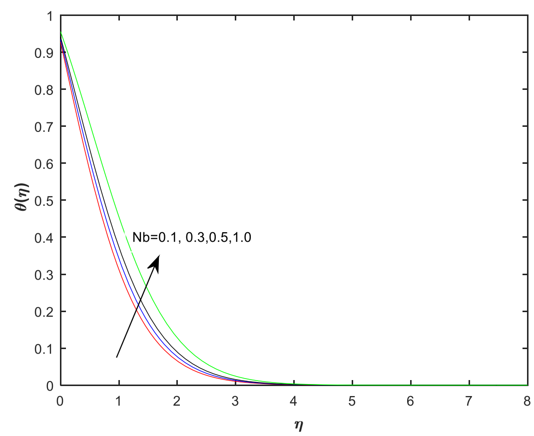

Figure 9: Temperature Profile for various values of Nb.

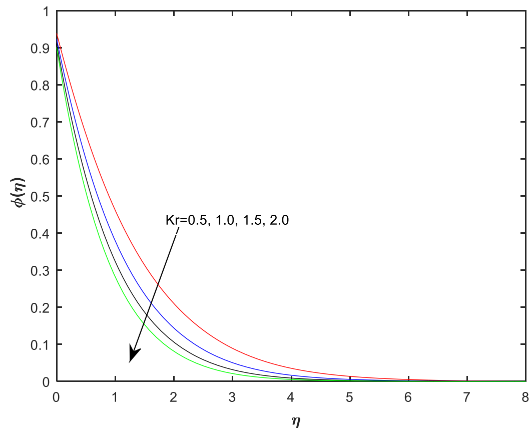

Figure 10: Concentration Profile for various values of Kr

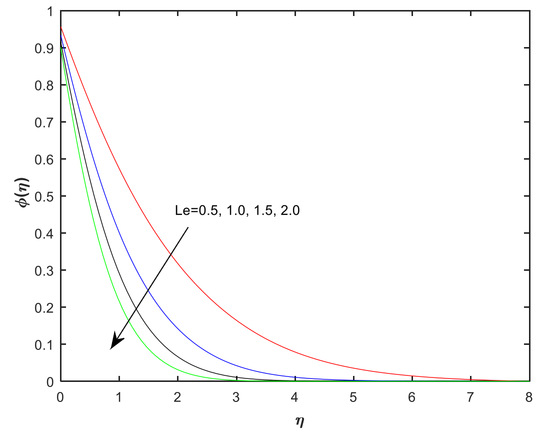

Figure 11: Concentration Profile for various values of Le

Table 1: The estimates of skin friction factor, Nusselt number, Sherwood number for different values of B,Q,Nt,Nb,Kr,Le,L_1,L_2,L_3 and S.

B	Q	Nt	Nb	Kr	Le	L_1	L_2	L_3	S	$-f''(0)$	$-\theta'(0)$	$-\phi'(0)$
0.5	0.1	0.1	0.1	0.1	0.1	0.1	0.1	0.1	0.1	0.953373	0.544371	0.755949
1										1.141595	0.557514	0.770805
1.5										1.235429	0.579709	0.795489
2										1.294181	0.524531	0.845122
0.1	-0.2	0.1	0.1	0.1	0.1	0.1	0.1	0.1	0.1	0.957215	0.523708	0.844095
	-0.1									0.957215	0.717854	0.928702
	0									0.957215	0.799153	1.002185
	0.1									0.957215	0.871248	1.057552
0.1	0	0.1	1	0.1	0.1	0.1	0.1	0.1	0.1	0.957215	0.190038	0.452225
		0.3								0.957215	0.287873	0.479390
		0.5								0.957215	0.352388	0.488595
		1								0.957215	0.439895	0.495879
0.1	0	0.1	0.1	0.1	0.1	0.1	0.1	0.1	0.1	0.957215	0.439895	0.452225
			0.3							0.957215	0.585888	0.512357
			0.5							0.957215	0.550337	0.581223
			1							0.957215	0.717854	0.928702
0.2	0	0.1	11	0.5	0.1	0.1	0.1	0.1	0.1	0.957215	0.000001	0.514295
				1						0.957215	0.000001	0.759525
				1.5						0.957215	0.000001	0.891445
				2						0.957215	0.000002	0.993955
0.2	0	0.1	11	0.1	0.5	0.1	0.1	0.1	0.1	0.957215	0.000000	0.437074
					1					0.957215	0.000000	0.553544
					1.5					0.957215	0.000001	0.842443
					2					0.957215	0.000004	0.993947
0.2	0	0.1	11	0.1	0.5	0.5	0.1	0.1	0.1	0.309825	0.000001	0.351835
						1				0.375415	0.000002	0.351417
						1.5				0.477157	0.000002	0.375832
0.2	0	0.1	11	0.1	0.5	0.5	0	0.1	0.1	0.558051	0.000003	0.400170
							0.5			0.957215	0.000002	0.270932
							1			0.957215	0.000042	0.313497
							1.5			0.957215	0.000308	0.371921
0.2	0	0.1	11	0.1	0.5	0.5	0.1	0	0.1	0.957215	0.001245	0.457090
								0.5		0.957215	0.000042	0.313497
								1		0.957215	0.000308	0.371921

								1.5		0.957215	0.001245	0.457090
0.2	0	0.1	11	0.1	0.5	0.5	0.1	0.1	0	0.942580	0.000003	0.407555
									0.5	1.020500	0.000012	0.551738
									1	1.113429	0.000033	0.728104
									1.5	1.225358	0.000071	0.899954

5. Conclusion

This study uses a chemical reaction on a stretchable sheet to explain the MHD slip effect and Casson upper convected Maxwell fluid stagnation point flow. The governing parameters, such as the velocity ratio, suction-injection parameter, Lewis numbers, Deborah number, magnetic field, Brownian motion parameter, thermophoresis parameter, chemical reactions parameter, thermal radiation parameter, velocity slip parameter, thermal slip parameter, singular slip parameter, Casson fluid parameter, and heat source parameter. The information about this paper is shown as follows:

- The effect of the magnetic field parameter's increase on the velocity field is lessened.
- The velocity field increases with rising magnetic field, while it decreases with rising solutal slip values.
- Concentration profiles are decreased by enhancing the values of Brownian motion, chemical reaction, Lewis number, thermal slip parameter, and singular slip parameter.
- The characteristics of velocity profiles with regard to changes in the suction parameter lead to a weakening of the velocity field.

Conflict of interests

None

Author Contribution

The authors contributed equally to this work, from the implementation and design of the research, the analysis of the results and to the writing of the manuscript.

Funding

The authors received no financial support for the research, authorship, and publication of this article.

References

1. Raju, C.S.K., Sandeep,N, Sugunamma, V, Jaya Chandra Babu, M and Ramana Reddy, J.V: Heat and mass transfer in magnetohydrodynamic Casson fluid over an exponentially permeable stretching surface, *Engineering science and Technology, an International Journal* 19(2015),45-52.
2. Raju, C.S.K., Sandeep,N and Saleem,S: Effects of induced magnetic field and homogeneous-heterogeous reactions on stagnation flow of a Casson fluid, *Engineering science and Technology, an International Journal* 19(2015),875-887.
3. Raju, C.S.K and Sandeep,N: Unsteady three-dimensional flow of casson-carreau fluids past a stretching surface, *Alexandria Engineering Journal*(2015)55, 1115-1125.
4. Sudipta. G and Swathi, M: MHD slip flow and heat transfer of casson nanofluid over an exponentially stretching permeable sheet, International journal of Automotive and Mechanical Engineering (2017)4,4785-4804.
5. Kumaran, G, Sandeep,N and Animasun,I.L: Computational modeling of magnetohydrodynamic non-Newtonian fluid flow past a paraboloid of revolution, *Alexandria Engineering Journal*(2017).
6. Sobamowo, G, Adesina, O,A and Lawrence Jayesimi: Magetohydrodynamic flow of dissipative casson-carreau nanofluid over a stretching sheet embedded in a porous medium under the influence of thermal radiation and variable internal heat generation:Engineering and Applied science letters(2019), DOI 10.30538/psrp-easl2019.0018.
7. Santosh, H,B, Mahesha and Raju, C.S.K: Unsteady carreau-casson fluids over a radiated shrinking sheet in a suspension of dust and graphene nanoparticles with non-fourier heat flux, *Nonlinear Engineering* (2019)8, 419-428.
8. Naga Santoshi,P, Ramana Reddy,G,V and Padma.P : Numerical Scrutinization of three dimensional casson-carreau nano fluid flow, *Journal of Applied and computational Mathematics*(2020)5, 531-542.
9. Macha, M and Kishan, N: finite element analysis of MHD viscoelastic nanofluid flow over a stretching sheet with radiation.*Process Eng*.(2015),432-439. http://doi.org/10.1015/j.proeng.2015.11.393.
10. Madhu, M,Kishan,Nand Champka,A,J: Boudary layer flow and heat transfer of a nonofluid over a non-linearly stretching sheet, *Int.J.Numerical Methods Heat fluid flow*(2015),25(7),2198-2217, http://doi.org/10.1108/HFF-02-2015-0055.
11. Macha, M ,Kishan, N and Champka,A,J: MHD flow of a non-Newtonian nanofluid over a non-linearly stretching sheet in the presence of thermal radiation with heat source/sink. *Eng.Comput*(2015)33(5),1510-1525,http://doi.org/10.1108/Ec-05-2015-0174.
12. Srinivas, C, Reddy, Kishan, N,Macha, M: Finite element analysis of Eyring-powell nano fluid over an exponential stretching sheet, *Int. J.Appl. Comput Math*(2017),4(8), 1-13, http://doi.org/10.1007/s40819-017-0438-x.
13. Macha, M and Kishan, N : MHD flow and heat transfer of casson nanofluid flow over a wedge, *Mech. Ind* (2017) ,18,210, http://dx.doi.org/http://doi./10.105/mecal/2015030.
14. Macha, M , Kishan, N and Champka,A,J: Unsteady flow of a Maxwell nanofluid over a stretching surface in the presence of magnetohydrodynamic and thermal radiation effects, *Propulsion Power Res* (2017), 5(1), 31-40,http://doi.org/10.1015/j.jppr2017.01.002.
15. JayachandraBabu,M, Sandeep, N : MHD non-Newtonian fluid flow over aslendering stretching sheet in the presence of cross-diffusion effects, *Alexandria Eng J* (2015), 55, 2193-2201, http://doi.org/10.1015/j.aej.2015.05.009.
16. Ramana Reddy, J, V, Anantha Kumar, K, Sugunamma, V and Sandeep,N : Effects of cross diffusion on MHD non-Newtonian fluids flow past a stretching sheet with non-uniform heat source/sink investigated, *Alexandria Eng. J* (2018), 57, 1829-1838,http://10.1015/j.aej.2015.05.009.
17. Tian, X,Li and B, Hu, Z: Convective stagnation point flow of a MHD non-Newtonian nano fluid towards a stretching plate,*Int.J. Heat Mass Transf* (2018), 127,758-780.
18. Nasir, S, Islam, S, Gul,T,Shan, Z, Khan,M. A, Khan,A,Z and Khan, S : Three-dimensional rotating flow of MHD single wall carbon nanotubes over a stretching sheet in presence of thermal radiation, *ApplNanosci*(2018), 8, 1351-1378.

19. Khan,N,s, Zuhra, S, Shah, Z, Bonyah, E,Khan, W and Islam, S :Eyring-powell slip flow of nano liquid film containing graphene nano particles(2018), *AIP ADV*, 8,115302.

20. Imran, M,A, Riaz, M,B, Shah, N,A and Zafar,A : Bounadry layer flow of MHD generalized Maxwell fluid over an exponentially accelerated infinite vertical surface with slip and Newtonian heating at the boundary(2018), *Results In Phys*., 8, 1051-1057, http://doi.org/10.1015/j.rinp.2018.01.035.

21. Elbashbeshy, E,M, A, R, Abdelgaber, K,M and Asker,H,G : Heat and mass transfer of a Maxwell nanofluid over a stretching surface with variable thickness embedded in porous medium(2018),*Int, J, Math. Comput.Sci*, 4(3), 85-98, http://www.aiscience.org/journal/ijmcs.

22. Rahbari, A, Addasi, M, Rahimipetroudi, I, Sunden, B, Ganji, D.D and Gholami, M, Heat transfer and MHd flow of non-Newtonian Maxwell fluid through a parallel plate channel (2018), *Mechsci*, 9,51-70, http://doi.org/105194/ms-9-51-2018.

23. Gireesha, B,J, Mahantesh, B,Subba, R, Gorla, R and Krupalakshmi, K, L : Mixed convection two-phase flow of Maxwell fluid under the influence of non-linear thermal radiation non-uniform heat source/sink and fluid-particle suspension (2018).*Ain. Shams Eng J*, 9,735-745, http://doi.org/10.1015/J.asej.2015.04.020.

24. Ghaffari, A, Javed, T and Labropulu, F : Oblique stagnation point flow of a non-Newtonian nano-fluid over a stretching surface with radiation (2017),*Therm Sci*. 21(5), 2139-2153.

25. Yasin, A,Bandari, S and Srinivasulu, T: Numerical solution of stagnation point flows of nano fluid due to an inclined stretching sheet(2018),*Int,J, ComputEng Res*, 8(2), 2250-3005.

26. Manjula, D and Jayalakshmi, K : Slip effects on unsteady MHD and heat transfer flow over a stretching sheet embedded with suction in a porous medium filled with a Jeffrey fluid(2018), *Int, J, Res*, 7(8), 509-523, http://doi.org/10.1515/ijnsns.2015-0055.

27. Aziz, M,A and Afify, A,A : Influences of slip velocity and induced magnetic field on MHD stagnation-point flow and heat transfer of casson fluid over a stretching sheet (2018), *Math ProblEng*,http://doi.org/10.1155/2018/9402835.

28. Ibrahim,S,M, Lorenzini,G, Vijaya, K, P and Raju, C, S,K: Influence of chemical reaction and heat source on dissipative MHD mixed convection flow of a casson nanofluid over a nonlinear permeable stretching sheet (2017), *Int, J, Heat Mass Transf*, 111, 345-355.

29. Lu, D, C , Ramzan, M, Bilal, M, Chung, J, D and Farooq, U: A numerical investigation of 3D MHD rotating flow with binary chemical reaction, activation energy and non-Fourier heat flux(2018) ,*CommunTheor Phys*,70,89-95, http://doi.org/10.1088/0253-5102/70/1/89.

30. Sreedevi G., Prasada Rao D.R.V., Makinde O.D., Venkata Ramana Reddy G. (2017), 'Soret and dufour effects on MHD flow with heat and mass transfer past a permeable stretching sheet in presence of thermal radiation', Indian Journal of Pure and Applied Physics, 55(8), PP.551-553.

31. Vedavathi N., Dharmaiah G., Balamurugan K.S., Prakash J. (2017), 'Heat transfer on mhd nanofluid flow over a semi infinite flat plate embedded in a porous medium with radiation absorption, heat source and diffusion thermo effect', Frontiers in Heat and Mass Transfer, 9(38), PP.-

32. Dhanalakshmi M., Reddy K.J., Ramakrishna K. (2017), 'Chemical reaction and soret effects on radiating MHD boundary layer flow over a moving vertical porous plate with heat source', Journal of Advanced Research in Dynamical and Control Systems, 9(), PP.2155-2155.

33. Hymavathi T., Sridhar W.(2018), 'Numerical study of flow and heat transfer of casson fluid over an exponentially porous stretching surface in presence of thermal radiation', International Journal of Mechanical and Production Engineering Research and Development ,8(4), PP. 1145-1154

34. Hari Krishna,Y, Ramana Reddy,G.V. and Oluwole Daniel Makinde.,(2018) Chemical reaction effect on MHD flow of Casson fluid with porous stretching sheet, *Defect and Diffusion Forum,* Vol.389, 100-109.